

University of Nebraska - Lincoln

DigitalCommons@University of Nebraska - Lincoln

Publications from USDA-ARS / UNL Faculty

U.S. Department of Agriculture: Agricultural
Research Service, Lincoln, Nebraska

2019

Quantification of Macrophages and Mycobacterium avium Subsp. paratuberculosis in Bovine Intestinal Tissue During Different Stages of Johne's Disease

Caitlin J. Jenvey

USDA-ARS, National Animal Disease Center & La Trobe University, Bundoora

Jesse M. Hostetter

Iowa State University, jesseh@iastate.edu

Adrienne L. Shircliff

USDA-ARS, National Animal Disease Center, adrienne.shircliff@usda.gov

John Bannantine

USDA ARS National Animal Disease Center, john.bannantine@usda.gov

Judith R. Stabel

USDA-ARS, National Animal Disease Center, jstabel@nadc.ars.usda.gov

Follow this and additional works at: <https://digitalcommons.unl.edu/usdaarsfacpub>

 Part of the [Agriculture Commons](#)

Jenvey, Caitlin J.; Hostetter, Jesse M.; Shircliff, Adrienne L.; Bannantine, John; and Stabel, Judith R., "Quantification of Macrophages and Mycobacterium avium Subsp. paratuberculosis in Bovine Intestinal Tissue During Different Stages of Johne's Disease" (2019). *Publications from USDA-ARS / UNL Faculty*. 2458.

<https://digitalcommons.unl.edu/usdaarsfacpub/2458>

This Article is brought to you for free and open access by the U.S. Department of Agriculture: Agricultural Research Service, Lincoln, Nebraska at DigitalCommons@University of Nebraska - Lincoln. It has been accepted for inclusion in Publications from USDA-ARS / UNL Faculty by an authorized administrator of DigitalCommons@University of Nebraska - Lincoln.

Quantification of Macrophages and *Mycobacterium avium* Subsp. *paratuberculosis* in Bovine Intestinal Tissue During Different Stages of Johne's Disease

Veterinary Pathology
2019, Vol. 56(5) 671–680
© The Author(s) 2019
Article reuse guidelines:
sagepub.com/journals-permissions
DOI: 10.1177/0300985819844823
journals.sagepub.com/home/vet



U.S. government works are not subject to copyright.

Caitlin J. Jenvey^{1,*} , Jesse M. Hostetter², Adrienne L. Shircliff¹,
John P. Bannantine¹ , and Judith R. Stabel¹ 

Abstract

Johne's disease is an enteric disease caused by the intracellular pathogen *Mycobacterium avium subsp. paratuberculosis* (MAP). Upon ingestion of MAP, it is translocated across the intestinal epithelium and may be killed by intestinal macrophages, or depending on the bacterial burden and immunological status of the animal, MAP may thwart innate defense mechanisms and persist within the macrophage. This study aimed to determine the numbers of macrophages and MAP present in bovine midileal tissue during different stages of infection. Immunofluorescent (IF) labeling was performed on frozen bovine midileal intestinal tissue collected from 28 Holstein dairy cows. The number of macrophages in midileal tissue sections was higher for clinically affected cows, followed by subclinically affected cows and then uninfected control cows. Macrophages were present throughout the tissue sections in clinical cows, including the tunica muscularis, submucosa, and the lamina propria around the crypts and in the villous tips, with progressively fewer macrophages in subclinically affected and control cows. Clinically affected cows also demonstrated significantly higher numbers of MAP and higher numbers of macrophages with intracellular MAP compared to subclinically affected cows. MAP IF labeling was present within the submucosa and lamina propria around the crypts, progressing into the villous tips in some clinically affected cows. Our findings indicate that number of macrophages increases with progression of infection, but a significant number of the macrophages present in the midileum are not associated with MAP.

Keywords

cattle, intestine, macrophage, *Mycobacterium avium subsp. paratuberculosis*, Johne's disease, granulomatous inflammation

Macrophages are key phagocytic cells in the innate immune response to bacterial pathogens that engulf bacteria such *Mycobacterium avium subsp. paratuberculosis* (MAP).²⁶ The gastrointestinal (GI) system contains the largest reservoir of tissue macrophages in the body, which are located within the subepithelial lamina propria.²⁰ It is generally considered that tissue macrophages originate from bone marrow stem cells that are differentiated into monocytic cells in the presence of cytokines and growth factors.²⁰ Monocytes are recruited from the circulation into the intestine via constitutive expression of transforming growth factor- β (TGF- β) and interleukin (IL)-8 by epithelial cells and mast cells.²⁰ Upon maturation of monocytes into tissue macrophages, these cells may survive for weeks to months and may actively recruit additional monocytes in the event of inflammation.² However, recent studies have also indicated that not all intestinal macrophages are replenished via blood monocytes. Self-maintaining macrophages that colonize specific niches of the GI tract (neuronal, blood vessels, gut-associated lymphoid tissue [GALT], and Paneth cells) during embryonic life have been identified. These self-maintaining

macrophages demonstrate distinct transcriptional profiles that reflect their localization and the ability of these macrophages to perform specialized functions dependent upon their environmental niche.¹⁰

The role of intestinal macrophages is to regulate the inflammatory response to bacteria and antigens, as well as protect the mucosa against pathogen entry while removing apoptotic cells

¹USDA—Agricultural Research Service (ARS), National Animal Disease Center, Ames, IA, USA

²Department of Veterinary Pathology, College of Veterinary Medicine, Iowa State University, Ames, IA, USA

*Current affiliation: Department of Animal, Plant and Soil Sciences, AgriBio Centre for Agribioscience, La Trobe University, Bundoora, Victoria, Australia.

Supplemental material for this article is available online.

Corresponding Author:

Judith R. Stabel, USDA—Agricultural Research Service (ARS), National Animal Disease Center, 1920 Dayton Rd, Ames, IA 50010, USA.

Email: judy.stabel@ars.usda.gov

and debris.²⁰ Progression of infection from an acute to a chronic state relies on the ability of the infecting pathogen to circumvent the killing processes of the macrophage. MAP is such a pathogen that has developed strategies to avoid macrophage degradation by preventing phagolysosome fusion and acidification,^{1,5} as well as macrophage activation.^{1,4,5} Yet only 10% to 15% of cattle exposed to MAP develop clinical disease,¹ suggesting that the bovine immune system is capable of controlling MAP infection. It is possible that the number of monocytes that are recruited to the intestine in response to MAP infection may play a significant role in the low numbers of cattle that develop clinical disease, but factors such as host health and genetics, environmental conditions, and infectious dose also contribute to the ability of an animal to control infection.¹ To date, there has been no published research on the effect of disease status on the number of macrophages present in the intestine and the relationship of macrophage number with intracellular MAP. This study aimed to use immunofluorescence (IF) and confocal microscopy to determine the number of macrophages, the number of MAP, and the number of macrophages with intracellular MAP present within frozen bovine midileal tissue of cows classified as having subclinical and clinical Johne's disease, compared to uninfected control cows.

Methods

Animals

Samples of midileal tissue were collected at necropsy from a total of 20 Holstein dairy cows naturally infected with MAP and 8 uninfected control cows. Cows were maintained as part of a herd housed at the National Animal Disease Center (NADC, Ames, IA) and were placed in 3 groups consisting of 8 noninfected healthy cows, 10 cows that were subclinically affected, and 10 cows with the clinical form of the disease with an average age of 7 (range, 3–10), 7 (range, 3–13), and 5.7 (range, 4–9) years, respectively. Control uninfected cows used in the present study were obtained from accredited JD-free herds and/or raised onsite from test-negative dams. Infected animals were either purchased from herds known to be positive for Johne's disease or were replacement animals born onsite to infected dams. Infected animals were naturally infected with MAP and were classified into the subclinical and clinical categories based upon fecal shedding, determined by fecal culture and polymerase chain reaction (PCR), and clinical signs.²² Subclinical cows were asymptomatic and intermittently shed low numbers of MAP in their feces, whereas clinical cows shed >100 colony-forming units (CFU)/g of feces and demonstrated clinical signs, including weight loss and intermittent diarrhea. Infected and control cows were housed separately and were tested at least biannually while housed at the NADC, with end-point testing just prior to necropsy.²⁴ Prior to necropsy, infection was monitored bacteriologically for fecal shedding of MAP using fecal culture and PCR as previously described,²² as well as serologic tests, such as Herdchek enzyme-linked

immunosorbent assay (ELISA) for serum antibodies (IDEXX, Westbrook, ME) and a modified MAP-specific interferon- γ (IFN- γ) assay measured in the plasma (Bovigam; Thermo Fisher Scientific, Carlsbad, CA).²⁵ There was no recorded evidence of any other health issues for cows used in this study that would affect the results. All uses of animals in this study were approved by the Institutional Animal Care and Use Committee (NADC).

Tissue Collection and Processing

At necropsy, the entire section of ileum extending from the ileocecal valve through the distal flange was excised and then cut equally into proximal, mid, and distal sections. Tissues were rinsed with 0.15 M phosphate-buffered saline (PBS) and cut into multiple cross sections for culture of MAP and PCR to assess bacterial burden. Cross sections immediately adjacent were processed for histopathology and IF labeling. A dry ice bath was prepared by combining 95% ethanol with dry ice and mixed until a slurry consistency was achieved. Isopentane (Sigma-Aldrich, St. Louis, MO) was added to a tin cup, and the cup was placed into the dry ice bath. The midileal intestinal samples were washed with PBS, pH 7.4, and a cross section was positioned luminal side down on a section of liver covered with Tissue-Tek optimum cutting temperature (OCT) compound (Sakura Finetek, Torrance, CA) to protect the villi during the freezing process and to ascertain tissue orientation postfreezing. The intestine-liver sample was wrapped in foil and placed in the isopentane for at least 5 minutes. The snap-frozen sample was transferred to dry ice for transport to storage at -80°C , where it remained until tissue sectioning could be performed.

The midileal intestinal samples were removed from -80°C and placed in a cryostat at -20°C for at least 30 minutes prior to sectioning. Tissue samples were embedded in OCT, cut in 6- μm sections, and adhered to ColorFrost Plus microscope slides (Thermo Fisher Scientific, Carlsbad, CA). Tissue sections were allowed to air-dry overnight at room temperature before fixing for 5 minutes at -20°C . Tissue sections were stored at -80°C until histochemistry and IF staining could be performed.

Histochemistry

Serial sections of frozen midileal tissue were stained with Harris hematoxylin and eosin (HE), Ziehl-Neelsen (ZN) for staining of acid-fast bacteria, and auramine O (AO) for staining of mycobacteria, following fixation in 1:1 acetone methanol for 5 minutes at -20°C .

HE staining was performed using a Leica autostainer (Leica Biosystems, Buffalo Grove, IL). Briefly, frozen slides were equilibrated to room temperature and rehydrated in deionized water for 5 minutes. Slides were then placed in Harris hematoxylin for 5 minutes, rinsed in a deionized water bath for 5 minutes, and dipped in acid alcohol, followed by another rinse in a deionized water bath for 5 minutes. Sections were then placed in 70% alcohol for 1 minute and then placed in eosin

solution for 10 to 15 seconds to stain the cytoplasm. Slides were then dehydrated in 95% alcohol, twice for 1 minute each, followed by 100% alcohol 3 times for 1 minute each. Sections were then cleared using Propar 3 times for 5 minutes each and coverslipped.

For ZN and AO staining, frozen slides were equilibrated to room temperature and rehydrated in deionized water for 5 minutes. For the ZN protocol, slides were placed in carbol fuchsin solution for 60 minutes at room temperature. Slides were decolorized in stock acid alcohol until sections appeared pale pink (approximately 10 seconds). Slides were then washed in a running water bath for 5 minutes. Slides were then placed in a Leica autostainer to counterstain with Harris hematoxylin for 5 minutes, followed by a brief rinse in a running water bath, and then coverslipped. For the AO protocol, slides were placed in auramine O solution for 10 minutes, washed in water, and then placed in 10% ferric chloride solution for 5 minutes. Slides were washed in water again, followed by counterstain in acridine orange, washing, and coverslipping.

Pathological Assessment of Acid-Fast Bacteria and Lesions

Each section was evaluated in a random order with treatment group blinded to the operator, with each field read at 200 \times and 20 fields per section. A scale from 0 to 5 was used for extent of granulomatous inflammation and acid-fast (AF) MAP bacilli as adapted from Palmer et al¹⁹ and used in Stabel et al.²³ Scores (0, granulomas/AF bacteria were not detected; 1, rare granulomas/AF bacteria were present in a section; 2, a granuloma with AF bacteria was typically present in each field) went up to a score of 5 in which granulomas and AF bacteria were diffusely present and replaced most of the architecture. Type of granuloma in the tissue section was designated as diffuse type (DIFFUSE) with nearly all of the lamina propria and submucosa involved or multifocal type (MULTI) with multiple fairly well-delineated aggregates. In each section, the location of MAP bacilli was designated as lamina propria (LP), submucosa (SM), Peyer's patches (PP), or submucosal lymphatic vessels (LYMPHATIC). NA was used to identify "not applicable" results.

Immunofluorescence Protocol

Tissue sections were removed from -80°C and allowed to equilibrate to room temperature for 10 to 20 minutes. A liquid blocker "Pap" pen was used to draw a hydrophobic barrier around the tissue and allowed to dry. Following tissue rehydration, 3,3'-diaminobenzidine (DAB; Vector Laboratories, Burlingame, CA) was added for 10 minutes to quench eosinophil autofluorescence and washed 3 times for 5 minutes each. A 10% horse serum was incubated for 30 minutes to reduce non-specific labeling. The slides were not washed between serum blocking and primary antibody incubation. The primary antibodies used in this study were a monoclonal mouse antibody to a macrophage surface antigen (clone AM-3 K; Abnova, Taipei,

Taiwan), diluted 1:200, and a polyclonal rabbit antibody to MAP cell wall protein (CWP), diluted 1:1000 (NADC). Antibody clone AM-3K has been demonstrated to specifically label tissue macrophages in a number of species, including cattle.^{29,30} The colocalization of AM-3K was compared to an antibody to bovine CD163 (clone LND68A; Washington State Monoclonal Antibody Center, Pullman, WA) to counter previous reports that the AM-3K clone was specific for CD163.¹⁶ Based upon the colocalization assessment, AM-3K was determined to be a good marker of the total macrophage population and not just the M2 phenotype as previously suggested (Suppl. Figs. S1, S2). The polyclonal rabbit MAP-CWP antibody has been demonstrated to specifically label MAP in bovine tissue.²¹ The primary antibodies were fluorescently labeled with an Alexa Fluor 555 goat anti-mouse IgG₁ and a cross-adsorbed Alexa Fluor 647 goat anti-rabbit IgG, respectively (ThermoFisher Scientific, Carlsbad, CA). Both secondary antibodies were diluted 1:1000. The primary and secondary antibodies were incubated for 60 minutes each at room temperature in a humidified chamber, followed by a washing step as described previously, and incubation with a 1:6000 dilution of 4',6-diamidino-2-phenylindole, dihydrochloride (DAPI) for 10 minutes. The slides were mounted in ProLong Gold Antifade Mountant (Thermo Fisher Scientific) and Richard-Allen Scientific "Slip-Rite" Cover Glass #1.5 (Thermo Fisher Scientific). The mounting medium was allowed to cure for at least 30 minutes at room temperature before imaging. Negative controls using omission of the primary or the secondary antibody were included with each protocol.

Confocal Imaging

The tissue sections were examined with an A1 Resonance Plus inverted microscope (Nikon, Melville, NY) equipped with a 4-laser gallium-arsenide-phosphide/normal photomultiplier tube detector unit (DU4) (GaAsP: 488 and 561; PMT: 405 and 640), Galvano resonant scanner, and NIS Elements Advanced Research software (version 4.50.00, Nikon Instruments, Melville, NY). Images were acquired by sequential scanning to avoid fluorescence crossover using a 405/488/561/640 dichroic mirror. All slides were imaged using the following bandpass filters: 405-nm solid-state diode laser and 450/50-nm bandpass filter, 488-nm solid-state diode laser and 525/50-nm bandpass filter, 561-nm solid-state diode laser and 600/50-nm bandpass filter, and 640-nm solid-state diode laser and 685/70-nm bandpass filter. All images were captured using a 60 \times Plan Apo lambda objective (1024 \times 1024 pixels), numerical aperture 0.75, pinhole 1.2 AU, and exposure 6.2 seconds per pixel dwell. Detector sensitivity (gain) and laser power settings were kept the same for all collected images to allow comparisons between markers and cows. A total of 10 images were collected per cow to perform statistical analysis.

Upon collection of each image, thresholding was performed to create a binary layer for each laser channel. The lower and upper intensity limits were thresholded to reduce the contribution of nonspecific IF labeling to binary layer calculations. In

addition, binary layer contours were smoothed and cleaned to remove small objects and reconstruct morphology. Following binary layer thresholding, the Field Measurement function in the Automated Results window was selected to calculate the area (number of macrophages/number of MAP) for each fluorescent marker for each image. To determine the numbers of macrophages with intracellular MAP, the area of MAP IF labeling that overlapped with macrophage IF labeling was also measured. Area was measured in μm^2 with the field for each image averaging $200 \mu\text{m}^2$. A total of 10 images were collected from the tissue of each cow with a total of 100 images per group. All data were collated in Microsoft Excel (Microsoft, Redmond, WA) prior to statistical analysis.

Statistical Analysis

Frequency histograms and Q-Q plots determined that the data were nonnormally distributed with a positive skew. A $\log + 1$ transformation was performed to achieve normally distributed data. Mean \pm 95% confidence intervals for number of macrophages, MAP, and macrophages with intracellular MAP were calculated for each cow and for each group (control, subclinical, clinical). An analysis of variance (ANOVA) with a post hoc Tukey's test was performed to determine significant differences in number ($\text{Pr} > F = 0.05$) between groups for each antibody and antibody colocalization. To determine differences between assessment of lesion and AF bacteria scores (categorical data only), a Fisher's exact test with 2-sided probability ($\text{Pr} < 0.05$) was calculated. Statistical analysis was performed using JMP version 8 (Cary, NC).

Results

Animals

Animals categorized as clinically affected had serum ELISA antibody titers averaging 2.45 S/P ratio, and fecal shedding averaged 2369 CFU of MAP/g feces. Cows subclinically affected were ELISA negative and averaged less than 17 CFU of MAP/g feces. Subclinically and clinically affected cows had positive antigen-specific IFN- γ results ($\text{Abs}_{450\text{nm}}\text{MPS} - \text{Abs}_{450\text{nm}}\text{NS} = 0.20 \pm 0.09$ and 0.20 ± 0.06 , respectively). In addition to fecal shedding and serologic analysis, clinical cows also showed physical signs of disease including weight loss and watery diarrhea, which provided further evidence for stratification of cows into groups.

Pathological Assessment

The lesions observed were typical for MAP-infected cattle (Figs. 1–3). In most subclinically affected cattle, no granulomas were identified. However, in 1 subclinically affected animal, there were rare small foci of macrophages in the villus tips (Fig. 2a). In clinically affected cattle, granulomas were present within the lamina propria and submucosa. Macrophages were commonly around submucosal lymphatic vessels. Two fairly distinct granuloma patterns were identified in clinically

affected cattle, which have previously been described.¹⁷ The first pattern was characterized by an extensive and diffuse infiltration of macrophages that distorted normal mucosal architecture. The second pattern consisted of multiple, fairly well-delineated clusters of macrophages that were separated by intact lamina propria and submucosa (Fig. 3a). Auramine O staining was consistent with AF staining (Figs. 1–3).

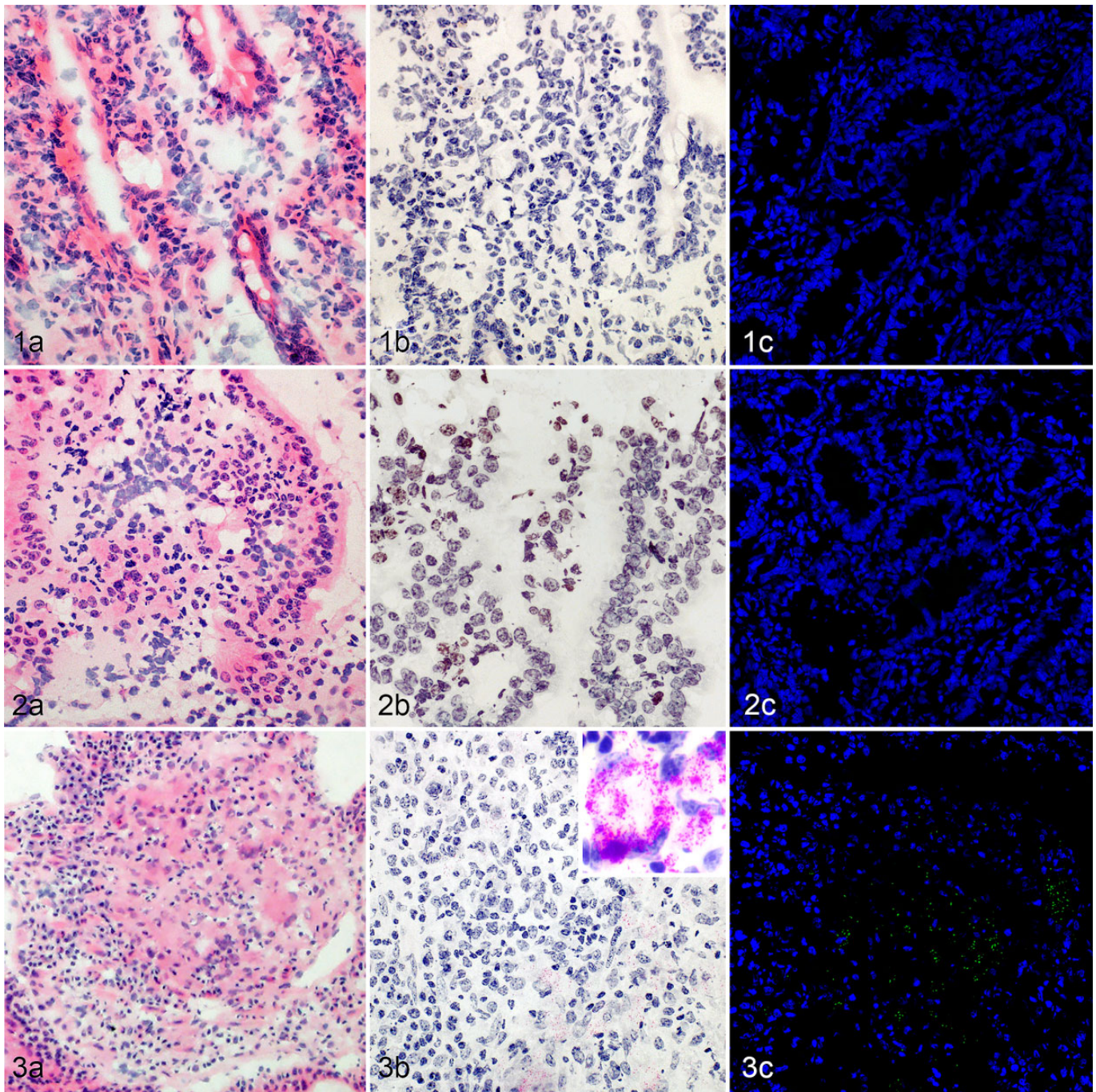
Acid-fast score, granulomatous inflammation score, and location of AF bacteria and granulomatous inflammation within midileal tissue are presented in Table 1. The exact probabilities for obtaining the observed frequencies for each category were significantly different between clinically and subclinically affected cows. However, there was no difference in probabilities among AF score, AF location, and granulomatous inflammation score (Table 1).

Location of IF Labeling

Immunofluorescent labeling of macrophages (clone AM-3 K) was observed in all control, subclinically, and clinically affected cows (Figs. 4–6). For control cows, most macrophages were located within the submucosa, with minimal IF labeling observed in the muscularis and the lamina propria around the crypts (Fig. 4). For subclinically affected cows, macrophages were observed within the submucosa and lamina propria surrounding the crypts, with increased numbers of macrophages toward the villus tips, as well as within the tunica muscularis (Fig. 5). For clinically affected cows, macrophages were observed within the submucosa and the lamina propria around the crypts and within the villus tips. Macrophages were also observed within the tunica muscularis, similar to subclinically affected cows (Fig. 6).

No MAP labeling was noted in images for control cows (Fig. 7; Suppl. Figs. S3–S10). For subclinically affected cows, IF labeling of MAP was observed in 12 out of 100 images (5/10 subclinically affected cows) (Fig. 8; Suppl. Figs. S11–S20) and in 84 out of 100 images in clinically affected cows (10/10 clinical cows) (Fig. 9; Suppl. Figs. S21–S30). For subclinically affected cows, the majority of MAP IF labeling was observed within the lamina propria around the crypts (Fig. 5). For clinically affected cows, MAP was observed within the submucosa and lamina propria around the crypts and, in some cows, had progressed entirely to the villus tips (Fig. 6).

Colocalization of MAP IF labeling with macrophage IF labeling was used to determine the numbers of macrophages with intracellular MAP. For subclinically affected cows, MAP IF labeling was observed in a total of 12 out of 100 images, and macrophage with intracellular MAP was observed in all 12 images. For clinically affected cows, MAP IF labeling was observed in 84 out of 100 images, and macrophages with intracellular MAP was observed in 77 out of 84 images. However, most macrophages observed in subclinically and clinically affected midileum were observed without intracellular MAP (Suppl. Figs. S11–S20 and S21–S30).



Figures 1–3. Midileal tissue, control cow. **Figure 1.** (a) There are no lesions. Hematoxylin and eosin (HE). (b) There is no *Mycobacterium avium* subsp. *paratuberculosis* (MAP). Acid-fast (AF). (c) There are no MAP. Auramine O (AO). **Figure 2.** MAP infection. (a) Subclinically affected cow with rare small foci of macrophages in the villus tips. HE. (b) No MAP are detected. AF. (c) No MAP are detected. AO. **Figure 3.** (a) Clinically affected cow with multiple, fairly well-delineated clusters of macrophages that are separated by intact lamina propria and submucosa. HE. (b) Multifocal aggregates of MAP (magenta). Inset: higher magnification. AF. (c) MAP (green) in the lamina propria. AO.

Number of Macrophages and MAP

The mean number of macrophages was significantly higher for clinically affected cows compared to both subclinically affected ($P = .0052$) and control cows ($P < .0001$). The mean number of macrophages for subclinically affected cows

was also significantly higher compared to control cows ($P = .0125$) (Table 2). The mean number of MAP was significantly higher for clinically affected cows compared to subclinically affected cows ($P < .0001$) (Table 2). The mean number of macrophages with intracellular MAP was significantly

Table 1. Pathological Assessment of Frozen Bovine Ileal Tissue.^a

Disease Form	AF Score					AF Location			Granulomatous Inflammation Score					Granulomatous Inflammation Location				
	0	1	2	3	4	5	NA	LP	LP/SM	0	1	2	3	4	5	NA	D	M
Control	8	0	0	0	0	0	8	0	0	8	0	0	0	0	0	8	0	0
Subclinical	10	0	0	0	0	0	10	0	0	7	1	0	0	0	0	9	0	1
Clinical	3	0	2	3	1	1	3	5	2	3	0	1	2	3	1	3	4	3
Fisher exact test	$P = .0031$					$P = .0031$			$P = .0198$					$P = .0031$				

Abbreviations: AF, acid fast; D, diffuse lesions; LP, lamina propria; LP/SM, lamina propria and submucosa; M, multifocal lesions; MAP, *Mycobacterium avium subsp. paratuberculosis*; NA, not applicable.

^aNumber of cows with different AF bacterial frequency scores, locations of AF bacteria, granulomatous inflammation scores, and types of granulomas in frozen bovine intestinal tissue, for control ($n = 8$), subclinically ($n = 10$), and clinically ($n = 10$) infected cows.

higher for clinically affected cows compared to subclinically affected cows ($P < .0001$) (Table 2).

The number of macrophages, MAP, and macrophages with intracellular MAP were compared across groups of animals based upon positive and negative pathology scores. Animals were categorized as having “negative pathology” if AF and granulomatous inflammation scores were 0 or if MAP location or granulomatous inflammation type was NA. All control and subclinically affected cows, as well as 3 of 10 clinical cows, were categorized with negative pathology. Of the cows categorized with negative pathology, clinically ($P = .0027$) and subclinically affected ($P = .0196$) cows had a significantly higher mean number of macrophages when compared to control cows (Table 3). In addition, clinically affected cows had significantly higher mean numbers of MAP ($P = .0257$) and macrophages with intracellular MAP ($P = .0005$) when compared to subclinically affected cows (Table 3). None of the control cows, 1 of 10 subclinically affected cows, and 7 of 10 clinically affected cows had granulomatous inflammation (ie, granulomatous inflammation scores ranging from 1–5). Clinically affected cows had significantly higher mean numbers of macrophages, mean numbers of MAP, and mean numbers of macrophages with intracellular MAP (Table 3) compared to subclinically affected cows. There were no significant differences between disease states for cows with positive AF scores, AF location, and granuloma type since positive scores were only obtained for clinically affected cows in this cohort of animals.

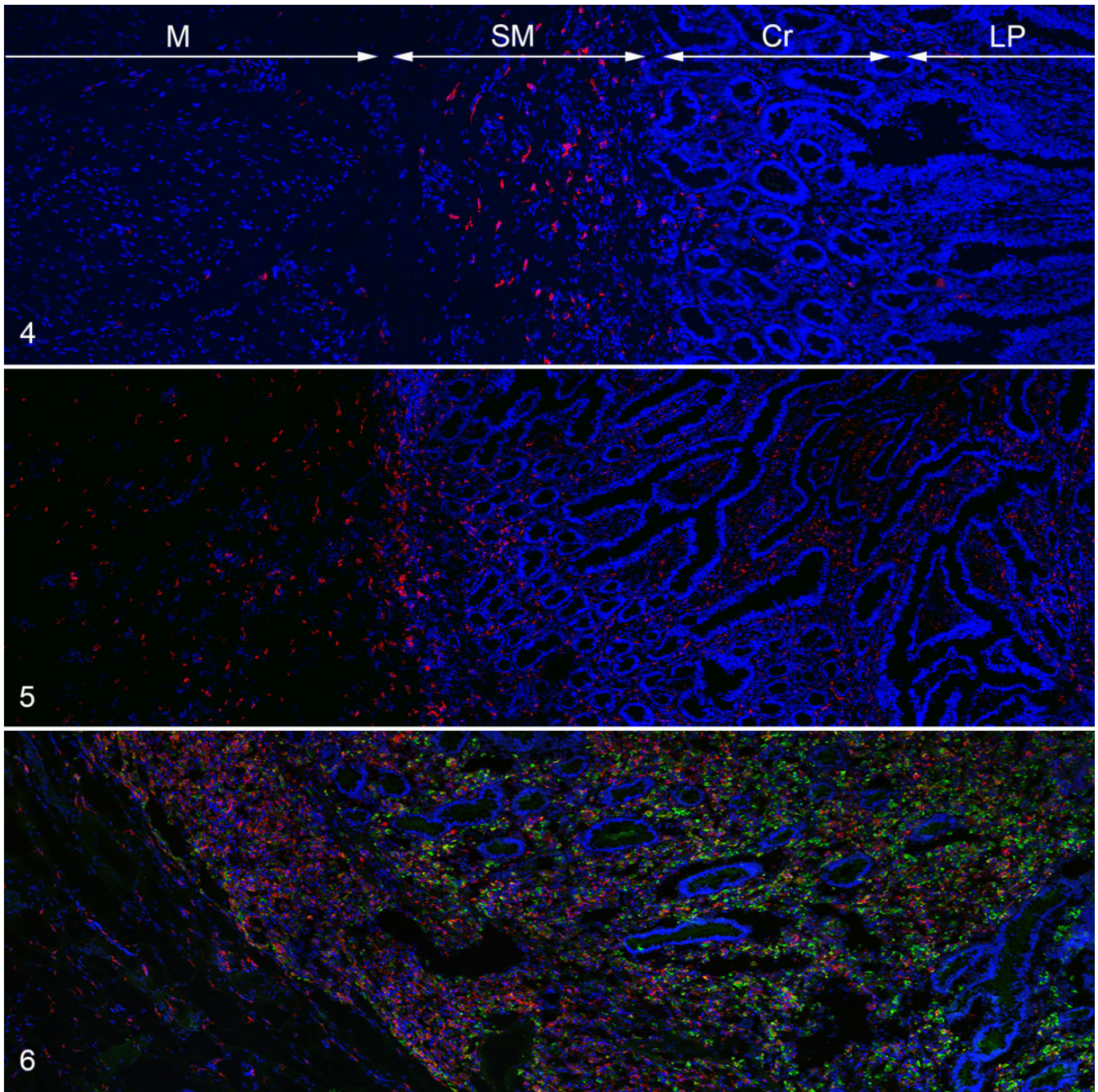
Discussion

Infection with MAP is characterized by a long subclinical infection period where animals intermittently shed low levels of MAP. Approximately 10% to 15% of infected animals will develop clinical disease,¹ which suggests that the bovine immune system has the ability to control the infection. Mononuclear phagocytes, such as monocytes and macrophages, are critical for protecting the host against invasion by MAP, but MAP can avoid degradation by preventing macrophage phagolysosome fusion and acidification.^{1,6,20} The purpose of the present study was to determine if macrophage numbers in the

midileum were affected by disease status in cows naturally infected with MAP and if the macrophages were positive for the presence of MAP, based upon the presence of MAP within the tissue. In addition to macrophage number, it was important to ascertain if disease state would affect the location of macrophages within the tissue, thereby affecting the ability to respond to an infectious pathogen such as MAP.

The clinically affected cows in the current study demonstrated significantly higher numbers of MAP, higher numbers of macrophages with intracellular MAP, and greater frequency of diffuse lesions in the intestine. Although the bovine innate immune system is capable of recruiting monocytes to the site of infection, these monocytes mature into intestinal macrophages and are capable of controlling MAP in the subclinical stage of infection. In contrast, macrophages present in the tissue of clinically affected cows are ultimately unable to clear MAP, resulting in increased recruitment of monocytes, progression of infection, and development of clinical disease. In addition, monocytes recruited to the tissue may proliferate within an intestinal environment geared toward Th2 immune responses to replenish tissue-resident macrophages. The ability of clinically affected cows to clear MAP is possibly due to the polarization of macrophages toward a particular phenotype, in particular, macrophage polarization toward a M2 phenotype, but that is beyond the scope of the present study.

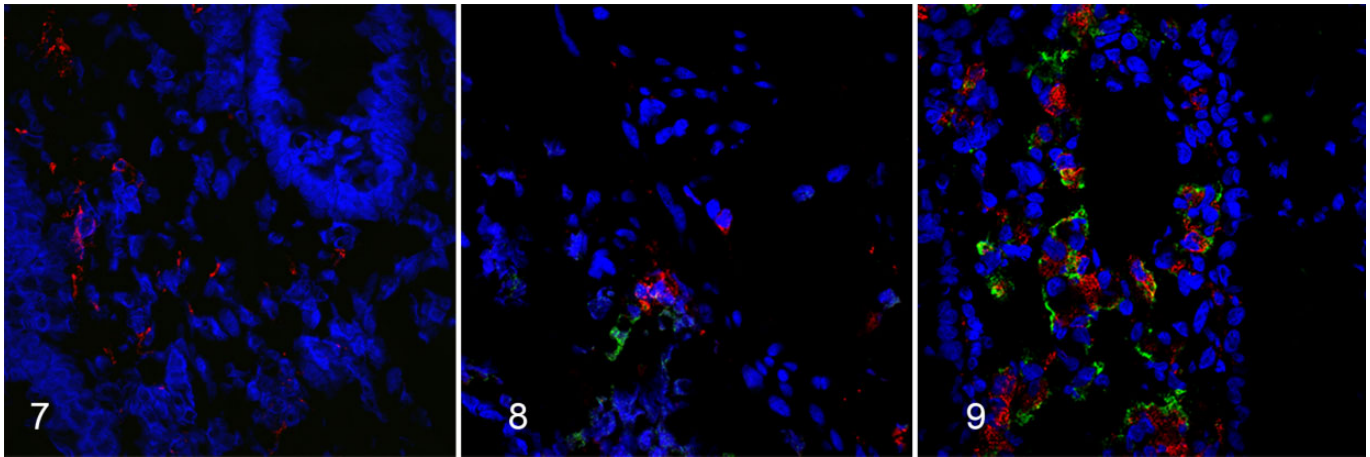
The location of macrophages observed in the intestinal tissue of the cows in the current study is consistent with prior studies of cattle infected with MAP. In cattle subclinically affected with MAP, small groups of macrophages have been demonstrated within the lamina propria and submucosa, while in clinically affected cattle, greater numbers of macrophages infiltrate the lamina propria and submucosa, as well as the tunica muscularis.^{6,7} Macrophages were also the dominant cell type observed at the site of infection.⁵ In a study by Magombedze et al,¹⁸ a mathematical prediction simulation model was created using data from naturally infected cows on retrospective fecal shedding and IFN- γ and serum antibody levels. Briefly, a hypothetical macrophage-based assay was developed using 3 models capturing Th1/IFN- γ and Th2/antibody immune response data and fecal shedding. Using a series of equations, they were able to capture the dynamics of uninfected



Figures 4–6. *Mycobacterium avium subsp. paratuberculosis* (MAP) infection, midileal tissue, bovine. Macrophages represented in red and MAP in green. Immunofluorescence. **Figure 4.** Control cow. Macrophages are present within the submucosa (SM), with some labeling of macrophages in the tunica muscularis (M) and the lamina propria (LP) around the crypts (Cr). No MAP is observed in control cows. **Figure 5.** Subclinically affected cow. Macrophages are present within the M, SM, and LP surrounding the Cr, with progression toward the villus tips. MAP is not observed in the present image but was present within the LP around the Cr in other images. **Figure 6.** Clinically affected cow. Macrophages are observed within the M, SM, and the LP around the Cr and within the villus. MAP are observed within the SM and LP around the Cr, and they progressed entirely into the villus in some cows.

and infected macrophages, along with free bacteria present, and use the presence of infected macrophages to predict disease and disease stages. They found that the simulated macrophage assay was a good predictor of latent infection associated with

subclinically affected cows, as well as subclinical animals that progress rapidly to clinical disease. In addition, they predicted that as the population of infected macrophages increases, as in clinical disease, the number of free MAP would accumulate as



Figures 7–9. *Mycobacterium avium subsp. paratuberculosis* (MAP) infection, midileal tissue, bovine. Macrophages represented in red and MAP in green. Immunofluorescence. **Figure 7.** Control cow, representative image. Only some macrophages are evident. **Figure 8.** Subclinically affected cow, representative image. Some macrophages are present and MAP present are in low number. **Figure 9.** Clinically affected cow, representative image. Macrophages are evident and MAP are present in high number.

Table 2. Numbers of Macrophages, MAP, and Macrophages With Intracellular MAP in Frozen Bovine Ileal Tissue Quantitated by Mean Area.^a

Characteristic	Mφ (μm ²)	MAP (μm ²)	Mφ With Intracellular MAP (μm ²)
Control	2.84 ± 0.09*	—	—
Subclinical	3.07 ± 0.17 [†]	0.21 ± 0.31 [†]	0.53 ± 0.76 [†]
Clinical	3.31 ± 0.18 [§]	1.63 ± 0.89 [§]	2.59 ± 0.51 [§]

^aMean area (log + 1 μm²) ± standard deviation for macrophages (Mφ), *Mycobacterium avium subsp. paratuberculosis* (MAP), and Mφ with intracellular MAP immunofluorescent labeling in frozen bovine intestinal tissue. Means with different superscript symbols within the same column are statistically different from one another using a significance level of .05.

the population of uninfected macrophages is depleted. In contrast, subclinical infections (slow persistent infection) were the result of lower macrophage infection rates, as the accumulation of extracellular bacteria is prevented by macrophages with the capacity to kill MAP and clear the infection.

In the current study, clinically affected cows demonstrated significantly higher numbers of macrophages compared to subclinically affected cows, but 99% and 80% of macrophages in these respective groups did not contain MAP. The high numbers of both uninfected macrophages and MAP observed in the clinically affected cows seem to suggest that accumulation of MAP was not inhibited by the presence of high numbers of uninfected macrophages. This is a critical observation and appears to directly affect whether the host will succumb to the disease. The ability of intestinal macrophages to eliminate a pathogen is directly related to their ability to produce proinflammatory cytokines and work in concert with local T cells, yet an intricate balance of macrophage responses is required within the intestine to reduce potential damage due to proinflammatory responses. This is done by a downregulation of inflammatory cytokines, as well as signal proteins such as

Table 3. Numbers of Macrophages, MAP, and Macrophages With Intracellular MAP in Bovine Ileal Tissue Based on Negative and Positive Pathology Scores.

Characteristic	Disease State		
	Control	Subclinical	Clinical
Macrophages^a			
AF score/AF location/GI type			
Negative	2.8 ± 0.1*	3.1 ± 0.2 [†]	3.3 ± 0.3 [†]
Positive	—	—	3.3 ± 0.2
GI score			
Negative	2.8 ± 0.1*	3.1 ± 0.2 [†]	3.3 ± 0.3 [†]
Positive	—	2.8 ± 0.0 [†]	3.3 ± 0.2 [§]
MAP^a			
AF score/AF location/GI type			
Negative	—	0.2 ± 0.3 [†]	0.8 ± 0.7 [§]
Positive	—	—	2.0 ± 0.7
GI score			
Negative	—	0.2 ± 0.3 [†]	0.8 ± 0.7 [†]
Positive	—	0.0 ± 0.0 [†]	2.0 ± 0.7 [§]
Macrophages with intracellular MAP^a			
AF score/AF location/GI type			
Negative	—	0.5 ± 0.8 [†]	2.3 ± 0.6 [§]
Positive	—	—	2.7 ± 0.4
GI score			
Negative	—	0.6 ± 0.8 [†]	2.3 ± 0.6 [§]
Positive	—	0.0 ± 0.0 [†]	2.7 ± 0.4 [§]

^aMean area (log + 1 μm²) ± standard deviation for immunofluorescent macrophage, *Mycobacterium avium subsp. paratuberculosis* (MAP), and macrophage with intracellular MAP labeling comparing negative and positive pathological assessments for acid-fast (AF) score, MAP location, granulomatous inflammation (GI) score, and GI type. Means with different superscript symbols within the same row are statistically different from one another using a significance level of .05.

MyD88, Toll/IL-1 (TIR)–domain containing adapter-inducing IFN-β adapter protein, and TRAF6 (tumor necrosis factor receptor-associated factor 6).²⁰ In the tissues of clinically

affected cows, as the MAP thwarts the killing ability of the macrophages and the downregulation of inflammatory responses occurs, more and more monocytes need to be recruited to perform this function. This aligns with the observations noted herein of high numbers of macrophages devoid of MAP.

As one would expect, a higher level of MAP IF labeling was observed in the intestinal tissue from clinically affected cows given the increased burden of intracellular MAP present. MAP was detected in the intestinal tissue of 50% of the subclinically affected cows compared to a 100% detection rate in tissues of clinically affected cows. The use of IF labeling improved the overall detection of MAP, regardless of disease state, when compared to AF score (0% subclinical and 70% clinical) in the current study. Although ZN staining is a quick and inexpensive method for the detection of AF bacteria, this technique has a variable sensitivity in fecal and tissue samples, identifying between 27% and 60% of clinically infected animals.^{8,9,13,14,27,28,31} A study by Coestsier et al⁹ also demonstrated stronger and more sensitive immunolabeling in bovine tissue using MAP-specific monoclonal antibodies when compared to ZN, which is consistent with the results of the current study. The success of ZN staining is dependent upon the intactness of the cell wall,⁹ the presence and type of lesions,⁹ and the type of tissue collected (inflamed vs noninflamed).¹⁵ Immunohistochemical methods of MAP detection in tissues are significantly more sensitive than AF staining, as they can identify fragmented and intact cell walls, free-floating mycobacterial antigens, and mycobacteria with defective cell walls.⁹ The polyclonal rabbit MAP-CWP antigen used in the current study has previously demonstrated a high binding affinity to MAP in bovine tissue.²¹ The MAP-CWP antibody demonstrated enhanced immunoreactivity in the cytoplasm of macrophages and giant cells, as well as extracellularly, and was superior to AF staining for the detection of low numbers of MAP in tissue.²¹ We believe that the use of this MAP-CWP antigen, in conjunction with immunofluorescence, demonstrates a more sensitive method for the detection of MAP in tissue, providing an accurate representation of the abundance of MAP in this particular cohort of naturally infected cows.

The presence of granulomatous lesions is a characteristic of infection with mycobacterial pathogens in cattle and has been well described for MAP infections.^{12,19} MAP infection induces granulomatous lesions within the lamina propria, including the presence of infected macrophages.¹¹ Five forms of granulomatous lesions have previously been described for cattle: focal, multifocal, diffuse multibacillary, diffuse paucibacillary, and diffuse intermediate,¹² with focal and multifocal lesions being most frequent in subclinically affected cattle and diffuse lesions most frequent in clinically affected cattle. The current study only observed multifocal and diffuse lesions, all of which were observed in clinically affected cows, with 4 of 10 clinically affected cows demonstrating diffuse-type lesions and 3 demonstrating multifocal-type lesions.

In contrast, only one subclinically affected cow in the present study had multifocal lesions whereas granulomas were not

identified in the others. Since the major cell type within a granulomatous lesion is the macrophage, this would support the greater number of macrophages observed in the tissues of clinically affected cows. Although peripheral immune responses have been correlated with the presence of lesions in the tissues of animals infected with MAP, a recent study by Fernandez et al¹¹ demonstrated that macrophages within different types of lesions within the intestine were shown to express different cytokines. Expression of different cytokines identifies the macrophage as a particular phenotype, and particular macrophage phenotypes have different roles, including host defense, tissue repair, and resolution of infection.⁶ Diffuse lesions were shown to align with M2 macrophages that express anti-inflammatory cytokines and are more likely to allow MAP to replicate within the macrophage. In contrast, multifocal lesions were shown to express proinflammatory cytokines more typical of M1 macrophages.¹⁰ The presence of both types of lesions in the tissues from cows characterized as clinically affected is supportive of macrophages with and without intracellular MAP.

Finally, a limitation of the current study may be the use of the AM-3 K antibody to label macrophages, as it remains possible that subsets of macrophages were not identified by this antibody and, therefore, were not included in the macrophage counts in this study. However, the use of any singular macrophage marker would present issues as some may capture dendritic cell populations (CD68), or skew toward a macrophage phenotype (M2, CD163), and others are inefficient for tissue macrophages (CD14).³ The AM-3 K antibody used herein was the most inclusive of the macrophage populations in our hands. In addition, the area calculation performed in this study is an estimate of the number of macrophages within a tissue section due to the difficulty of separating individual macrophage labeling. Thus, we were unable to determine if macrophage size (ie, macrophages enlarging after engulfing MAP) also changed with progression of infection. Therefore, the increased area (ie, number of macrophages) observed as infection progressed may not in fact be due to an increase in the numbers of anti-inflammatory macrophages, as suggested by Komohara et al,¹⁶ but rather an increase in size of macrophages.

Conclusions

The number of macrophages within frozen bovine midileal tissue sections of cows naturally infected with MAP was higher for clinically affected cows, lower in subclinically affected cows, and lowest in control cows. Macrophages were present in the submucosa and tunica muscularis in control cows as well as those cows subclinically and clinically affected with MAP. Subclinically and clinically affected cows also had macrophages in the deep lamina propria around the crypts, and clinically affected cows also had macrophages in the lamina propria of the villus tips. Compared to subclinically affected cows, clinically affected cows had significantly higher numbers of MAP and higher numbers of macrophages with intracellular MAP. Infected macrophages were mainly present within the

submucosa and the deep lamina propria, progressing into the villus tips in some clinically affected cows. In addition, only diffuse and multifocal-type lesions were observed in this cohort of naturally infected cows, the majority of which were observed in clinically affected cows. It is possible that the ability of clinical cows to clear MAP may be dependent upon the polarization of the macrophages toward a particular phenotype (M1 or M2) present within intestinal lesions.

Acknowledgements

We thank Ginny Montgomery and Judith Stasko of the National Animal Disease Center Histology and Microscopy Services Unit for their technical experience and expertise.

Declaration of Conflicting Interests


The author(s) declared no potential conflicts of interest with respect to the research, authorship, and/or publication of this article.


Funding

The author(s) disclosed receipt of the following financial support for the research, authorship, and/or publication of this article: This project was funded through the National Animal Disease Center, Agricultural Research Service, US Department of Agriculture.

ORCID iD

Caitlin J. Jenvey  <https://orcid.org/0000-0002-4052-4330>

John P. Bannantine  <https://orcid.org/0000-0002-5692-7898>

Judith R. Stabel  <https://orcid.org/0000-0001-9039-8582>

References

- Arsenault RJ, Maattanen P, Daigle J, et al. From mouth to macrophage: mechanisms of innate immune subversion by *Mycobacterium avium* subsp. *paratuberculosis*. *Vet Res*. 2014;**45**(1):54–68.
- Bain C, Mowat A. Macrophages in intestinal homeostasis and inflammation. *Immunol Rev*. 2014;**260**(1):102–117.
- Barros MHM, Hauck F, Dreyer JH, et al. Macrophage polarization: an immunohistochemical approach for identifying M1 and M2 macrophages. *PLoS One* 2013;**8**(11):e80908.
- Benoit M, Desnues B, Mege J-L. Macrophage polarization in bacterial infections. *J Immunol*. 2008;**181**(6):3733–3739.
- Buergelt CD, Hall C, McEntee K, et al. Pathological evaluation of paratuberculosis in naturally infected cattle. *Vet Pathol*. 1978;**15**(2):196–207.
- Cheville N, Hostetter J, Thomsen B, et al. Intracellular trafficking of *Mycobacterium avium* ss. *paratuberculosis* in macrophages. *Dtsch Tieraerztl Wochenschr*. 2001;**108**(6):236–242.
- Clarke CJ. The pathology and pathogenesis of paratuberculosis in ruminants and other species. *J Comp Pathol*. 1997;**116**(3):217–261.
- Coelho A, Pinto M, Miranda A, et al. Comparative evaluation of PCR in Ziehl-Neelsen stained smears and PCR in tissues for diagnosis of *Mycobacterium avium* subspecies *paratuberculosis*. *Indian J Exp Biol*. 2010;**48**(9):948–950.
- Coetsier C, Havaux X, Mattelard F, et al. Detection of *Mycobacterium avium* subsp. *paratuberculosis* in infected tissues by new-species-specific immunohistological procedures. *Clin Diagn Lab Immunol*. 1998;**5**(4):446–451.
- De Schepper S, Verheijden S, Aguilera-Lizarraga J, et al. Self-maintaining gut macrophages are essential for intestinal homeostasis. *Cell*. 2019;**176**(3):676.
- Fernandez M, Benavides J, Castano P, et al. Macrophage subsets within granulomatous intestinal lesions in bovine paratuberculosis. *Vet Pathol*. 2017;**54**(1):82–93.
- Gonzalez J, Geijo MV, Garcia-Pariente C, et al. Histopathological classification of lesions associated with natural paratuberculosis infection in cattle. *J Comp Pathol*. 2005;**133**(2–3):184–196.
- Hietala S. The options in diagnosing ruminant paratuberculosis. *Vet Med*. 1992;**87**:1122–1132.
- Huntley JFJ, Whitlock RH, Bannantine JP, et al. Comparison of diagnostic detection methods for *Mycobacterium avium* subsp. *paratuberculosis* in North American bison. *Vet Pathol*. 2005;**42**(1):42–51.
- Imirzalioglu C, Dahmen H, Hain T, et al. Highly specific and quick detection of *Mycobacterium avium* subsp. *paratuberculosis* in feces and gut tissue of cattle and humans by multiple real-time PCR assays. *J Clin Microbiol*. 2011;**49**(5):1843–1852.
- Komohara Y, Hirahara J, Horikawa T, et al. AM-3 K, an anti-macrophage antibody, recognizes CD163, a molecule associated with an anti-inflammatory macrophage phenotype. *J Histochem Cytochem*. 2006;**54**(7):763–771.
- Lei L, Plattner B, Hostetter J. Live *Mycobacterium avium* subsp. *paratuberculosis* and a Killed-Bacterium vaccine induce distinct subcutaneous granulomas, with unique cellular and cytokine profiles. *Clin Vaccine Immunol*. 2008;**15**(5):783–793.
- Magombedze G, Shiri T, Eda S, et al. Inferring biomarkers for *Mycobacterium avium* subsp. *paratuberculosis* infection and disease progression in cattle using experimental data. *Sci Rep*. 2017;**7**:44765.
- Palmer MV, Waters WR, Thacker TC. Lesion development and immunohistochemical changes in granulomas from cattle experimentally infected with *Mycobacterium bovis*. *Vet Pathol*. 2007;**44**(6):863–874.
- Smith PD, Smythies LE, Shen R, et al. Intestinal macrophages and response to microbial encroachment. *Mucosal Immunol*. 2011;**4**(1):31–42.
- Stabel JR, Ackerman MR, Goff JP. Comparison of polyclonal antibodies to three different preparations of *Mycobacterium paratuberculosis* in immunohistochemical diagnosis of Johne's disease in cattle. *J Vet Diagn Invest*. 1996;**8**(4):469–473.
- Stabel JR, Bradner L, Robbe-Austerman S, et al. Clinical disease and stage of lactation influence shedding of *Mycobacterium avium* subspecies *paratuberculosis* into milk and colostrum of naturally infected dairy cows. *J Dairy Sci*. 2014;**97**(10):6296–6304.
- Stabel JR, Palmer MV, Harris B, et al. Pathogenesis of *Mycobacterium avium* subsp. *paratuberculosis* in neonatal calves after oral or intraperitoneal experimental infection. *Vet Microbiol*. 2009;**136**(3):306–313.
- Stabel JR, Reinhardt TA, Hempel RJ. Short communication: vitamin D status and responses in dairy cows naturally infected with *Mycobacterium avium* ssp. *paratuberculosis*. *J Dairy Sci* 2019;**102**(2):1594–1600.
- Stabel JR, Whitlock R. An evaluation of a modified interferon-gamma assay for the detection of paratuberculosis in dairy herds. *Vet Immunol Immunopathol*. 2001;**79**(1–2):69–81.
- Tooker BC, Burton JL, Coussens PM. Survival tactics of *M. paratuberculosis* in bovine macrophage cells. *Vet Immunol Immunopathol*. 2002;**87**(3–4):429–437.
- Weber MF, Verhoeff J, van Schaik G, et al. Evaluation of Ziehl-Neelsen stained faecal smear and ELISA as tools for surveillance of clinical paratuberculosis in cattle in the Netherlands. *Prev Vet Med*. 2009;**92**(3):256–266.
- Woodbury MR, Chirino-Trejo M, Mihajlovic B. Diagnostic detection methods for *Mycobacterium avium* subsp. *paratuberculosis* in white-tailed deer. *Can Vet J*. 2008;**49**(7):683–688.
- Yamate J, Yoshida H, Tsukamoto Y, et al. Distribution of cells immunopositive for AM-3K, a novel monoclonal antibody recognizing human macrophages, in normal and diseased tissues of dogs, cats, horses, cattle, pigs and rabbits. *Vet Pathol*. 2000;**37**(2):168–176.
- Zeng L, Takeya M, Ling X, et al. Interspecies reactivities of anti-human macrophage monoclonal antibodies to various animal species. *J Histochem Cytochem*. 1996;**44**(8):845–853.
- Zimmer K, Drager K, Klawonn W, et al. Contribution to the diagnosis of Johne's disease in cattle: comparative studies on the validity of Ziehl-Neelsen staining, faecal culture and a commercially available DNA-Probe test in detecting *Mycobacterium paratuberculosis* in feces from cattle. *J Vet Med B/Zentralbl Veterinaermed B*. 1999;**46**(2):137–140.